Interstitial ordering of nitrogen and carbon in laser nitrided and laser carburized austenitic stainless steel

2006 J. Phys.: Condens. Matter 18 10561

(http://iopscience.iop.org/0953-8984/18/47/004)

INSTITUTE OF PHYSICS PUBLISHING JOURNAL OF PHYSICS: CONDENSED MATTER

J. Phys.: Condens. Matter **18** (2006) 10561–10570 doi:10.1088/0953-8984/18/47/004

Interstitial ordering of nitrogen and carbon in laser nitrided and laser carburized austenitic stainless steel

H Binczycka[1,2], M Kahle[1], S Cusenza[1], E Carpene[3] and P Schaaf[1]

[1] Universität Göttingen, II Physikalisches Institut, Friedrich-Hund-Platz 1, 37077 Göttingen, Germany
[2] Jagiellonian University, M Smoluchowski Institute of Physics, 30-059 Krakow, Poland
[3] Politecnico di Milano, Dipartimento di Fisica, piazza Leonardo da Vinci 32, 20133 Milano, Italy

E-mail: pschaaf@uni-goettingen.de

Received 6 September 2006, in final form 23 October 2006
Published 8 November 2006
Online at stacks.iop.org/JPhysCM/18/10561

Abstract

The distribution of carbon and nitrogen atoms on the octahedral interstitial sites of the face-centred-cubic austenite phase in Fe–C and Fe–N alloys, especially in austenitic stainless steel, is still causing controversy. In this work, results of Mössbauer experiments are presented in order to advance the understanding of this interstitial occupation. Therefore, laser carburized and laser nitrided austenitic stainless steel was investigated by means of x-ray diffraction and Mössbauer spectroscopy. Three subspectra in terms of different iron sites were resolved in the Mössbauer spectra for these iron–carbon and iron–nitrogen austenites. The isomer shifts, the quadrupole splittings and in particular the subspectra fractions depend on the type of the introduced atom and undergo changes when increasing the carbon or nitrogen content. This is discussed in connection with the existing ordering models for interstitial atoms. No clear evidence could be found for a perfect random occupation, nor for a perfect ordered occupation of the interstitials. Nevertheless, there seems to a tendency for a weak attractive interaction for nitrogen interstitials, and for a stronger repulsive force for the carbon interstitials in laser nitrided/carburized austenitic stainless steel.

1. Introduction

Irradiation of surfaces with short laser pulses in reactive atmospheres (here nitrogen and methane) can lead to very effective nitriding or carburization via complicated laser–surface–gas–plasma interactions [1]. Laser nitriding is used for the fast and easy production of nitride coatings on iron, iron alloys, and other metals. Here, the results of the laser nitriding process and of the laser carburization applied to austenitic stainless steel, i.e. the nitrogen and carbon

take-up from the ambient gas upon irradiation with short laser pulses, are presented and discussed in connection with the interstitial ordering in the austenite.

In austenite the iron atoms are arranged in a close-packed face-centred-cubic (fcc) lattice, and the nitrogen and carbon atoms (N and C) occupy a limited number of the crystallographic equivalent octahedral interstitial sites [2]. The nitrogen austenite, or γ-Fe(N), is a well-known phase for Mössbauer spectroscopy. Nevertheless, the ordering of nitrogen interstitials as well as the proper fitting of the hyperfine parameters are still in discussion. In spite of the several attempts performed to obtain the interaction between atoms from the Mössbauer data [3–11] and the numerous articles on the distribution of solute atoms in the interstitial sites [12, 13], up to now, there has been no full understanding on the way the interstitial atoms are distributed.

This paper is focusing on the study of isomer shifts, quadrupole splittings and subspectra fractions of the Fe sites as a function of the content of incorporated nitrogen or carbon atoms in the austenite. The hyperfine parameters are compared with the results published so far [3–13].

2. Experiment

The austenitic stainless steel 1.4401 (AISI 316, X5CrNiMo18.10.3) was chosen for the treatments. This steel is a standard construction material used in many industrial applications. In addition, there was the interest in studying the possibly different behaviour of this fcc material compared to the pure iron studied so far.

The samples have been polished mechanically and then irradiated with a Siemens XP2020 pulsed excimer laser ($\lambda = 308$ nm, pulse duration 55 ns) either in a pure methane atmosphere (CH_4, purity 99.5%), or pure nitrogen (N_2, purity 99.999%), or pure ammonia (NH_3) at a pressure of 0.1 MPa (1 bar). The irradiation chamber has been previously evacuated to a pressure lower than 10^{-3} Pa to prevent oxidation and then filled with the desired ambient gas. The laser beam was set to a fluence of 3.7 or 4 J cm^{-2}. The whole sample surface was covered by a meandering scanning of the laser spot relative to the sample. Full experimental details are given elsewhere [14–16].

Conversion electron Mössbauer spectroscopy (CEMS) and conversion x-ray Mössbauer spectroscopy (CXMS) were applied simultaneously to the samples without any further treatment. All Mössbauer spectra were taken at room temperature with a ^{57}Co/Rh source with an activity of about 400 MBq and a constant acceleration drive. The conversion and Auger electrons were detected in a He/CH_4 gas-flow proportional counter and the conversion x-rays in a Ar/CH_4 gas-flow toroidal detector placed in front of the CEMS detector. The spectra were stored in a multichannel scaler with 1024 channels and fitted by a least squares fitting routine [17]. Velocity calibration was performed with a 25 μm α-Fe foil at room temperature, and all isomer shifts are related to the latter.

Additional analyses were carried out using x-ray diffraction (XRD) with Cu Kα radiation at a fixed incident angle of 5° in a Bruker AXS D8 machine.

3. Results

Seven samples with different carbon and nitrogen contents were selected for the present study. The carbon and nitrogen $c_{C/N}$ contents were determined from the XRD measurements. The XRD pattern of a laser nitrided austenitic stainless steel sample is shown in figure 1. One clearly sees the presence of two fcc phases with slightly different lattice constants a_e and a_0. No other reflections or phases could be observed.

After the laser nitriding or carburizing an additional fcc phase with an increased lattice parameter has formed, apart from the original fcc phase of the stainless steel. This additional

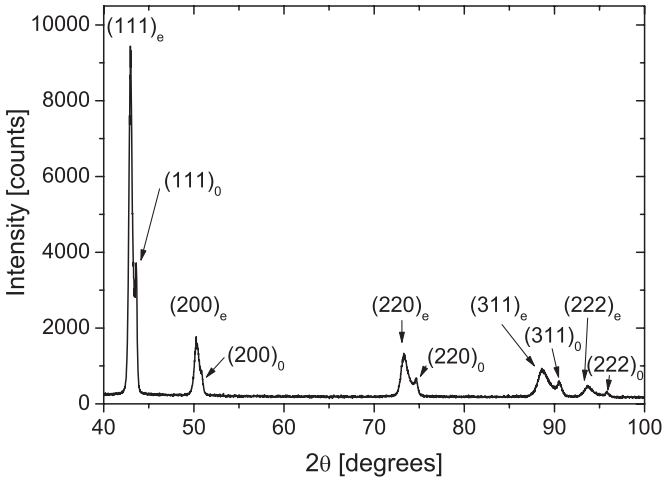

Figure 1. XRD pattern of laser nitrided austenitic stainless steel. Sample S6 measured with 5° fixed incidence angle. The reflections are indexed according to two fcc phases. Index '0' stands for the fcc phase of the virgin fcc steel. Index 'e' stands for the expanded austenite phase containing N or C formed by the laser treatment.

Table 1. Irradiation parameters (at 0.1 MPa atmosphere, number of laser pulses, and laser fluence H), lattice constants, carbon/nitrogen content of the samples.

No	Gas	Pulses	H (J cm^{-2})	a_0 (Å)	a_e (Å)	$c_{C,N}$ (at.%)	$y = c/(1-c)$
S1	—	—	—	3.5939(18)	—	0.00(10)	0.0000(10)
S2	CH_4	2 × 2	4.0	3.5988(30)	3.5992(49)	0.05(73)	0.0005(74)
S3	CH_4	4 × 4	4.0	3.5948(38)	3.6325(47)	4.83(77)	0.0508(86)
S4	CH_4	5 × 6	4.0	3.5995(11)	3.6445(33)	5.77(45)	0.0612(51)
S5	NH_3	11 × 12	3.7	3.5961(19)	3.6186(27)	2.88(42)	0.0297(45)
S6	N_2	11 × 12	3.7	3.5967(16)	3.6627(33)	8.46(47)	0.0924(56)
S7	N_2	16 × 16	3.7	3.5905(54)	3.6471(55)	7.27(99)	0.0782(115)

phase is sometimes called expanded austenite or γ-Fe(N, C) [4]. It can also be written as FeN_y or FeC_y. For the sake of simplicity, this shortened writing of the more correct form M(N, C) with M = Fe, Cr, Ni, or Mo is used here. This should not indicate a change in the overall alloy composition. Additional effects or interactions due to the alloying elements [11] should not occur here as well, because there is only a very short treatment time.

The actual $c_{C/N}$ content in the samples ($y = c/(1-c)$) was determined from the lattice parameter a_e extracted from the diffraction patterns with the known lattice parameter from the virgin austenite a_0 and using the empirical relation for austenite [18]:

$$a_e = a_0 + c_{N,C} \times 0.78 \text{ Å}. \quad (1)$$

The lattice parameters and the resulting concentrations $c_{C/N}$ obtained from the XRD analyses for the various samples are listed in table 1.

The CEMS spectrum of the untreated austenitic stainless steel is shown in figure 2. The original austenitic phase before the laser treatment can be fitted with a singlet S (isomer shift IS = −0.09 mm s^{-1}) and a doublet D_S (with IS = −0.09 mm s^{-1} and the quadrupole splitting QS = 0.19 mm s^{-1}) in agreement with values given in the literature [3–5]. The cubic structure of the non-magnetic phase should result in a single line only. Nevertheless, the alloying

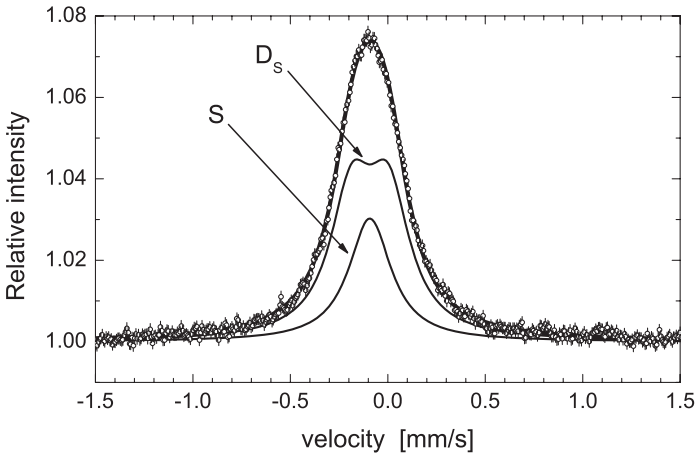

Figure 2. CEMS spectrum of the untreated austenitic stainless steel AISI 316 (sample S1). A singlet S and one doublet D_S are used for fitting the spectrum.

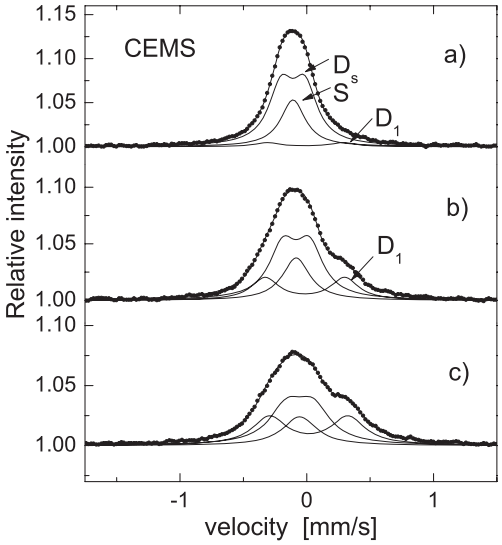

Figure 3. CEMS spectra of laser carburized stainless steel with various carbon contents: (a) S2—0.05 at.% C, (b) S3—4.8 at.% C, (c) S4—5.8 at.% C.

elements (Cr, Ni, Mo) cause a slight distortion of the cubic symmetry and thus result in a small quadrupole splitting [11].

After laser nitriding or laser carburizing an additional doublet D_1 has to be used for the fitting besides the S and D_S subspectra from the virgin austenitic stainless steel; figure 3 shows the CEMS spectra of laser carburized austenitic stainless steel with various carbon contents ($c_C = 0.05$, 4.8 and 5.8 at.%). For comparison the CXMS spectra for the same samples are shown in figure 4.

The fraction of the doublet D_1 for the CXMS spectra is considerably smaller as compared to the CEMS spectra. Taking into account the different information depths for both measurements (about 0.15 μm for CEMS and about 10 μm for CXMS) one can conclude

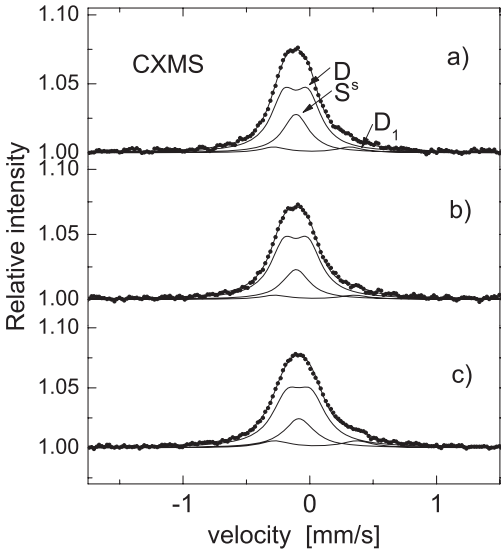

Figure 4. CXMS spectra of laser carburized austenitic stainless steel with various carbon contents: (a) S2—0.05 at.% C, (b) S3—4.8 at.% C, (c) S4—5.8 at.% C.

that the carburized phase is limited to the surface region with a transition to the virgin γ-Fe phase, present in deeper regions. The depth of the modified layer can be estimated to be in the order of 1 μm [14, 15].

The fitting procedure for the CEMS spectra was performed with the same values of isomer shift for singlet S and doublet D_S and with the same value of the linewidth Γ for all subspectra. For most of the samples the linewidth was $\Gamma = 0.25(2)$ mm s^{-1} and for the sample with the highest carbon content of 5.6 at.%, a linewidth of $\Gamma = 0.30(1)$ mm s^{-1} was obtained. The fits were obtained with χ^2 values between 0.50 and 0.61.

The CEMS spectra obtained after laser nitriding of austenitic stainless steel with nitrogen contents of $c_N = 2.9$, 8.5, and 7.3 at.% are shown in figure 5.

There is no difference in structure of the laser carburized and laser nitrided stainless steel spectra. The CEMS spectrum exhibits a superposition of the subspectra for the untreated stainless steel (S, D_S) and an additional doublet D_1 due to the nitrogen or carbon incorporation in the austenitic structure. The fitting procedure with an extra doublet D_2 (IS = 0.20 mm s^{-1}, QS = 0.70 mm s^{-1}, $A = 2(2)\%$) for the sample S6 with nitrogen content $c_N = 8.5$ at.% does not significantly improve the result.

Figure 6 shows the dependence of isomer shift (IS), quadrupole splitting (QS) and relative areas (A) for the (S + D_S) states and for the doublet D_1 on the content of the interstitial atoms incorporated into austenitic stainless steel. The parameters are in agreement with the results reported by Foct [6], Nadutov [11], Oda *et al* [7, 8], and Laneri *et al* [12] as given in table 2. The hyperfine parameters and the areas of the subspectra are summarized in figure 6.

The ratio of the areas of the singlet S to the doublet D_S does not vary significantly with the interstitial content $c_{C/N}$. Always an S/D_S area ratio of 0.43(4) is observed.

The isomer shifts for the Fe atoms attributed to (S + D_S) subspectra and to the doublet D_1 increase with increasing nitrogen and carbon content. This effect seems to be more systematic and more linear for nitrogen austenite. For the nitrogen case a linear relation of $IS_S = -0.087(7)$ mm s^{-1} + $y0.787(93)$ mm s^{-1} can be obtained (line in figure 6(a)). The

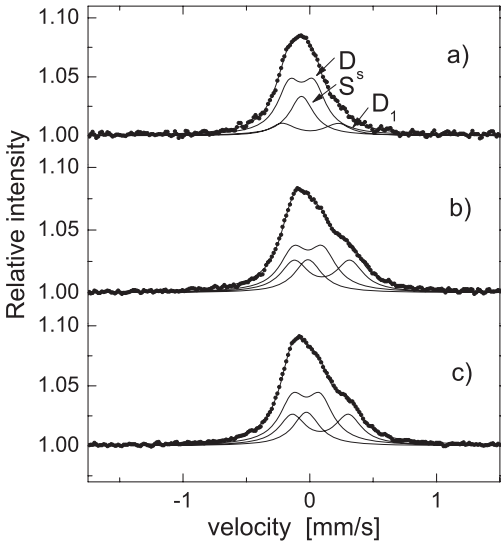

Figure 5. CEMS spectra of laser nitrided stainless steel with various nitrogen contents: (a) S5—2.9 at.% C, (b) S6—8.5 at.% C, (c) S7—7.3 at.% C.

Table 2. Isomer shift (IS), quadrupole splitting (QS) and relative fractions (A) of the corresponding Fe environments from the literature [6–8, 11, 12].

	S	D_1			D_2	
	IS	IS	QS	A	A	
y	(mm s^{-1})	(mm s^{-1})	(mm s^{-1})	(%)	(%)	Reference
			Fe–C System			
0.018	−0.143	−0.090	0.655	53		[11]
0.052	−0.07	−0.01	0.61	43		[12]
0.072	−0.05	0.01	0.61	48		[12]
0.082	−0.04	0.02	0.63	50		[12]
0.081	−0.05	0.00	0.67	45		[8]
			Fe–N system			
0.027	−0.085	−0.09	0.383	61	8	[11]
0.098	−0.10	0.15	0.25	75	2	[6]
0.099	0.01	0.08	0.39	50	3	[7]

same behaviour is found for the IS values of the doublet D_S. Again, only for the nitrogen case, a linear increase of IS can be found with $IS_{D_1} = -0.042(9)$ mm s$^{-1} + y \cdot 1.537(122)$ mm s^{-1} (line in figure 6(b)). The IS values of the doublet D_1 are more positive with respect to those of the singlet S and the doublet D_S in carbon austenite and in nitrogen austenite spectra. Furthermore, the linear coefficient for D_1 is almost twice that of S/D_S.

The QS value of the doublet D_S is slightly increasing when the carbon or nitrogen content increases. The relation $QS_{D_S} = 0.188(3)$ mm s$^{-1} + y \cdot 0.345(49)$ mm s^{-1} is obtained (line in figure 6(c)). The increase in the quadrupole splitting traces back to an increase in the electric field gradient, indicating that the charge inhomogeneity caused by the interstitial atom is increasing or coming closer to the Fe spy atom.

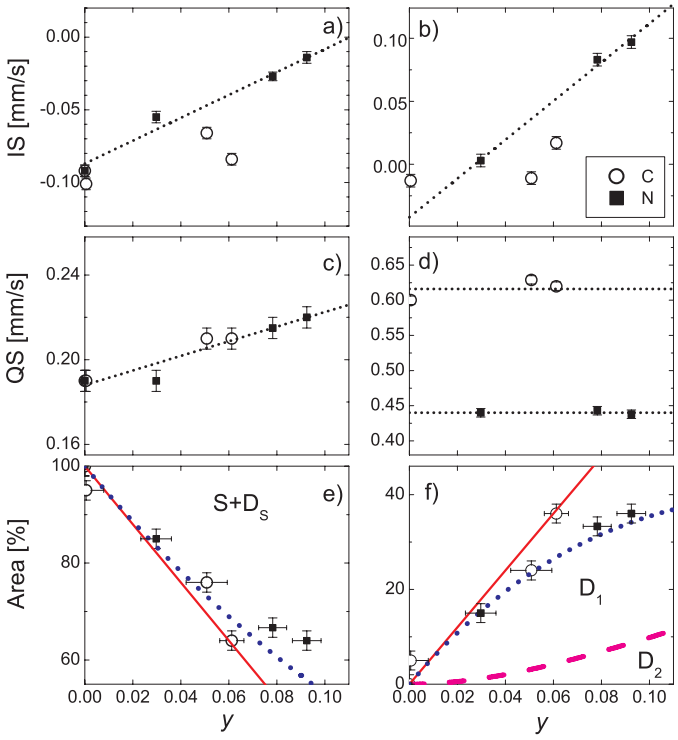

Figure 6. Isomer shift (IS), quadrupole splitting (QS) and relative area (A) of the subspectra for nitrided (■) and carburized (○) austenitic stainless steel versus the interstitial content y (i.e. the total fraction of the occupied interstitial sites). The lines in the IS and QS graphs indicate the dependence on the y value. The lines in the area graphs (e) and (f) correspond to the ordered (solid line) and random (dotted and dashed line) models explained in the text.

(This figure is in colour only in the electronic version)

The QS values of the doublet D_1 in the spectrum of the nitrogen austenite (QS = 0.440(2) mm s^{-1}) is considerably smaller than that of the doublet in carbon austenite (QS = 0.616(9) mm s^{-1}). They are both not changing with the carbon and nitrogen content.

The main difference is observed in the relative areas of the subspectra described by $S+D_S$ and D_1. A decreasing area for $S+D_S$ and correspondingly an increasing area for D_1 is observed for an increasing content of the interstitial atoms. This is discussed in the following section.

4. Discussion

In austenite the iron atoms are arranged in a close-packed face-centred-cubic (fcc) lattice, and the nitrogen and carbon atoms occupy a limited number of the crystallographically equivalent octahedral interstices located at the centre and at the mid-points of the edges of the unit cell [2]. In an alloy with $n_{N/C}$ nitrogen or carbon atoms and n_{Fe} iron atoms we have $y = n_{N/C}/n_{Fe}$. Then y and $1 - y$ represent the fraction of occupied and of empty interstitial sites, respectively [19, 20]. If we write the iron–nitrogen or iron–carbon austenite as FeN_y or FeC_y, with $y = c/(1 - c)$ where c is the nitrogen or carbon concentration, we have with y just the probability that a certain octahedral site is occupied by a nitrogen or carbon atom (if no ordering or blocking effects causes the sites to be inequivalent). This parameter y was used in

figure 6 to show how the hyperfine parameters depend on the nitrogen or carbon content in the austenite.

Mainly, two models have been proposed to describe the distribution of N and C atoms in the Fe–N and Fe–C austenite solutions. The first one assumes a random structure (RSM—random structure model) [3–8, 11, 12] and the second proposes an ordered structure (OSM—ordered structure model) [9, 10, 12]. According to previous analyses of Mössbauer spectra for fcc Fe–N and Fe–C solid solutions, the singlet S belongs to Fe atoms with no interstitial atoms in the first coordination shell. For austenitic stainless steel the subspectra S and D_S represent the pure stainless steel with no carbon or nitrogen neighbour. The quadrupole interaction D_1 arises from the distortion of the cubic symmetry due to the presence of the interstitial atom in the neighbourhood. Thus, the doublet D_1 describes iron atoms with one nearest neighbour interstitial atom. An iron atom with two interstitial nearest neighbours, where the latter form an angle of 90° (D_2-90) should result in the same quadrupole splitting and thus is not distinguishable from D_1 [3]. The contribution to the spectra of a doublet D_2-180 associated with Fe sites with two neighbouring atoms in a 180° configuration would have approximately a value of QS twice that of D_1. Such a doublet was not detected in our spectra within the error limits. The presence of this doublet depends on the type of interstitial atoms and on their content [3, 4, 12, 13].

The observed increase in the IS values of the Fe sites with no interstitial atoms in the first coordination shell and of the Fe sites related to a doublet D_1 for nitrogen austenite and for carbon austenite indicates a decrease in the charge density of s electrons. The electronic changes in Fe–N and Fe–C alloys were calculated using an *ab initio* norm-conserving pseudopotential method [21] and the full-potential linearized augmented-plane-wave LAPW method [22, 23] for the Fe_8X (X = C, N) ordered structure. The more positive values for the isomer shift of the doublet D_1 observed in the Mössbauer spectra for iron–nitrogen austenite than for those of the iron–carbon austenite is consistent with the LAPW calculations. The calculated isomer shift values of the different iron environments are $IS_{D1,N} = 0.021$ mm s^{-1} and $IS_{D1,C} = -0.038$ mm s^{-1}, respectively [13, 23]. The agreement between our experimental data and the calculated parameters is better for the iron–carbon austenite than for the iron–nitrogen austenite. This fact would support the random distribution of N atoms at the interstitial sites and a more ordered distribution for C atoms. However, suggestions from *ab initio* norm-conserving pseudopotential method calculations are just the opposite [21].

In general, the QS values in iron–carbon austenite are larger than in the iron–nitrogen case, probably due to a stronger influence of C atoms than that of N atoms which might be caused by the larger atomic radius of C compared to N and thus a larger overlap of the electron shells. Our data are in good agreement with the results reported in the literature [3–8, 11, 12]. In iron–carbon austenite, an ordering of carbon interstitials was proposed and observed, originating from a repulsive interaction of the carbon interstitials [9, 10]. The blocking of neighbouring interstitial sites by carbon atoms explains the absence of Fe atoms with two or more nearest neighbours C atoms in the iron–carbon austenite.

In iron–nitrogen austenite, no such repulsive forces are predicted and thus no ordering should occur. N atoms are smaller than C atoms and a random distribution of nitrogen atoms on the interstitial sites was proposed, only [3–8, 11, 12].

The analyses of the Mössbauer spectra show that the contributions of the subspectra ($S + D_S$) and D_1 in iron–nitrogen austenite and carbon–nitrogen austenite are quite similar. The relative areas for these two sites are in good agreement with the relative fractions obtained from a Monte Carlo simulation for the RSM [12, 24]. This fact suggests that the iron–carbon and the iron–nitrogen austenite do not differ markedly in their degree of randomness in the interstitial occupation of carbon and nitrogen. Nevertheless, there seems to be a significant

difference between carbon and nitrogen when looking to the fractions in figure 6. The solid line in figure 6 is drawn according to the ordering (blocking) model, where the probabilities p (set equal to the subspectra areas) are given by

$$p(\mathrm{S}+\mathrm{D_S}) = 1 - 6y; \qquad p(\mathrm{D_1}) = 6y. \tag{2}$$

It is seen that the carbon austenite quite nicely follows this behaviour. In contrast, the random order is represented by the dotted line in figure 6 and is calculated as a binomial distribution:

$$p(\mathrm{S}+\mathrm{D_S}) = \binom{6}{0} y^0(1-y)^{(6-0)} = (1-y)^6, \tag{3}$$

and for the doublet $\mathrm{D_1}$:

$$p(\mathrm{D_1}) = \binom{6}{1} y^1(1-y)^{(6-1)}. \tag{4}$$

It is seen that the nitrogen austenite better follows this line. The data are even a bit above this line, which would hint at a kind of agglomeration of nitrogen atoms in contrast to the carbon case where they seem to separate and follow the 'blocking' model line. We have more $\mathrm{S} + \mathrm{D_S}$ than the random model predicts, which suggests that the nitrogen interstitials like to go to sites where there is already a nitrogen atom in the neighbourhood. The dashed line in figure 6 predicts the occurrence of the $\mathrm{D_2}$ doublet, which we were not able to resolve unambiguously in the spectra. This might hint at a clustering of N interstitials, by avoiding the $\mathrm{D_2}$-180 configuration and favouring the $\mathrm{D_2}$-90 configuration.

Anyway, for a clear proof and explanation of this behaviour more data points have to be present, but the experimental values of the isomer shift compared to calculated parameters [23, 24] support the random distribution of N atoms in the interstitial sites and more ordered distribution for C atoms.

5. Conclusion

The Mössbauer spectra of laser carburized and laser nitrided austenitic stainless steel were resolved and analysed. The spectra reveal the presence of three sites for the Fe atoms with different local environments (S, $\mathrm{D_S}$, $\mathrm{D_1}$) depending on the incorporated atom. The hyperfine parameters of iron–nitrogen austenite and iron–carbon austenite are strongly dependent on the content of incorporated nitrogen or carbon in the austenitic stainless steel. The analyses of the Mössbauer spectra show that the contributions of subspectra ($\mathrm{S} + \mathrm{D_S}$) and $\mathrm{D_1}$ in iron–nitrogen austenite and carbon–nitrogen austenite are similar. The presented results indicate that the distribution of the nitrogen and carbon atoms in the interstitial sites of stainless steel could be not be described unambiguously with respect to the random and ordering models discussed. Nevertheless, there is a clear indication of a weak attractive interaction between the nitrogen interstitials and a stronger repulsive interaction between carbon interstitials in austenitic stainless steel.

Acknowledgment

One of the authors (HB) thanks the people at the Zweites Physikalisches Institut of the University of Göttingen for their hospitality and generous support.

References

[1] Bäuerle D 2000 *Laser Processing and Chemistry* (Berlin: Springer)
[2] Kaufman L, Radcliffe S V and Cohen M 1962 *Decomposition of Austenite by Diffusional Processes* ed V F Zackay and H I Aaronson (New York: Interscience) p 313

[3] Schaaf P, Illgner C, Niederdrenk M and Lieb K-P 1995 *Hyperfine Interact.* **95** 199
[4] Schaaf P, Lieb K-P, Carpane E, Han M and Landry F 2001 *Czech. J. Phys.* **51** 625
[5] Carpene E, Landry F, Han M, Lieb K-P and Schaaf P 2002 *Hyperfine Interact.* **139/140** 355
[6] Foct J, Rochegude P and Hendry A 1988 *Acta Metall.* **36** 501
[7] Oda K, Umezu K and Ino H 1990 *J. Phys.: Condens. Matter* **2** 10147
[8] Oda K, Fujimura H and Ino H 1994 *J. Phys.: Condens. Matter* **6** 679
[9] Bauer Ph, Uwakweh O N C and Genin J M R 1988 *Hyperfine Interact.* **41** 555
[10] Uwakweh O N C, Bauer Ph and Genin J M R 1990 *Metall. Trans.* A **21** 589
[11] Nadutov V M 1998 *Mater. Sci. Eng.* A **254** 234
[12] Laneri K, Desimoni J, Zarragoicoechea G J and Fernandez Guillermet A 2002 *Phys. Rev.* B **66** 134201
[13] Desimoni J 2004 *Hyperfine Interact.* **156/157** 505
[14] Illgner C, Schaaf P, Lieb K-P, Queitsch R and Barnikel J 1998 *J. Appl. Phys.* **83** 2907
[15] Landry F, Lieb K-P and Schaaf P 1999 *J. Appl. Phys.* **86** 168
[16] Schaaf P 2002 *Prog. Mater. Sci.* **47** 1
[17] Landry F and Schaaf P 1998 *GöMOSS—Windows Fitprogram for the Analysis of Mössbauer Spectra*
[18] Ruhl R C and Cohen M 1969 *Trans. Metall. AIME* **245** 241
[19] Lacher J R 1937 *Proc. R. Soc.* A **161** 525
[20] Fowler R and Guggenheim E A 1956 *Statistical Thermodynamics* (Cambridge: Cambridge University Press)
[21] Gavriljuk V G, Shanina B D and Berns H 2000 *Acta Mater.* **48** 3879
[22] Timoshevskii A N, Timoshevskii V A and Yanchistsky B Z 2001 *J. Phys.: Condens. Matter* **13** 1051
[23] Platzer E L, Blanca Y, Desimoni J and Christensen N E 2005 *Hyperfine Interact.* **161** 197–202
[24] Vergera L, Desimoni J, Fernandez Guillermet A and Zarragoicoechea G J 2004 *Hyperfine Interact.* **156/157** 531